Inorganic Chemistry

Article

pubs.acs.org/IC

Copper Iminopyrrolidinates: A Study of Thermal and Surface Chemistry

Jason P. Coyle,[†] Peter J. Pallister,[†] Agnieszka Kurek,[†] Eric R. Sirianni,[‡] Glenn P. A. Yap,[‡] and Seán T. Barry*[,†]

[†]Department of Chemistry, Carleton University, 1125 Colonel By Drive, Ottawa, Canada

[‡]Department of Chemistry & Biochemistry, University of Delaware, Newark, United States

ABSTRACT: Several copper(I) iminopyrrolidinates have been evaluated by thermogravimetric analysis (TGA) and solution based ^{1}H NMR studies to determine their thermal stability and decomposition mechanisms. Iminopyrrolidinates were used as a ligand for copper(I) to block previously identified decomposition routes of carbodiimide deinsertion and β-hydrogen abstraction. The compounds copper(I) isopropyl-iminopyrrolidinate (**1**) and copper(I) *tert*-butyl-iminopyrrolidinate (**2**) were synthesized for this study, and compared to the previously reported copper(I) *tert*-butyl-imino-2,2-dimethylpyrrolidinate (**3**) and the copper(I) guanidinate $[Me_2NC(^iPrN)_2Cu]_2$ (**4**). Compounds **1** and **2** were found to be volatile yet susceptible to decomposition during TGA. At 165 °C in C_6D_6, they had half-lives of 181.7 h and 23.7 h, respectively. The main thermolysis product of **1** and **2** was their respective protonated iminopyrrolidine ligand. β-Hydrogen abstraction was proposed for the mechanism of thermal decomposition. Since compound **3** showed no thermolysis at 165 °C, it was further studied by chemisorption on high surface area silica. It was found to eliminate an isobutene upon chemisoption at 275 °C. Annealing the sample at 350 °C showed further evidence of the decomposition of the surface species, likely eliminating ethene, and producing a surface bound methylene diamine.

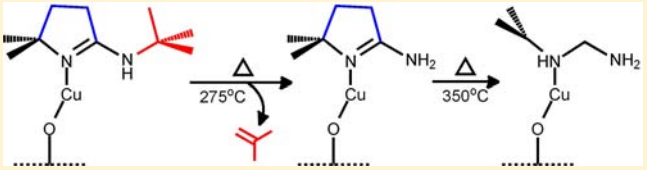

INTRODUCTION

Copper metal remains an interesting topic for chemical vapor deposition (CVD) and atomic layer deposition (ALD) because of its use in microelectronics, primarily as an interconnect.[1] One class of particularly well-studied precursors are the amidinates, which originated from the Gordon group in the early 2000s.[2] Copper amidinates have utility in ALD[2a] and CVD[3] processes between temperatures of 150−240 °C when using hydrogen as a reducing agent. Copper(I)-*N*,*N*′-di-isopropylacetamidinate has been shown to undergo CVD deposition as low as 140 °C,[4] and produces free amidine, acetonitrile, propene, and iminopropane when allowed to thermally decompose in the absence of a reducing agent.[5] These findings have been corroborated in the surface study work of copper(I) acetamidinates on nickel where—above 130 °C—the self-limiting nature of the monolayer is compromised and continuous uptake of the copper precursor is observed. Similar ligand fragments were identified in the surface work as in the gas phase work.

We have previously investigated the thermal decomposition of copper(I) guanidinates, which are similar to amidinates except that the exocyclic group is an amide, rather than an alkyl.[6,7] Using a guanidinate with isopropyl groups on the chelating nitrogens, we found two distinct thermal decomposition mechanisms (Figure 1). In solution at lower temperatures, the guanidinate deinserted carbodiimide (CDI) and produced the parent amine of the exocyclic amide group.[6] In the gas phase at greater than 150 °C, the methylene carbon

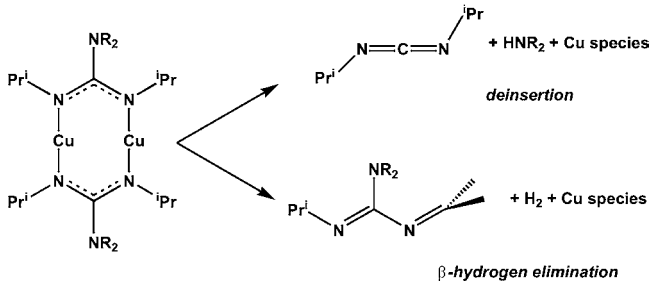

Figure 1. Two thermal decomposition pathways for a copper(I) guanidinate species.

of the isopropyl group on the chelating nitrogen loses a hydrogen and produces an oxidized guanidine. Hydrogen gas is also found as a thermolysis side product.[7]

Both of these thermal decomposition mechanisms are troubling from the point of view of developing a copper precursor for ALD. In the first case, the elimination of the oxidized guanidinate by β-hydrogen abstraction produces a copper hydride, which readily eliminates dihydrogen or parent guanidine to produce copper metal. This circumscribes an ALD process in favor of a CVD process. CDI deinsertion also greatly limits the use of this precursor in thermal processes. The formation of a (transient) copper-amide bond creates a species

Received: September 27, 2012
Published: January 3, 2013

   dx.doi.org/10.1021/ic3021035 | *Inorg. Chem.* 2013, 52, 910−917

that will readily decompose,[8] thus also preventing ALD in favor of a CVD process.

A redesign of the basic amidinate framework is necessary to remove the known thermal decomposition pathways of this ligand family. Our group has developed and extensively characterized a novel iminopyrrolidinate ligand family that has evidenced good thermal stability. Recently, we have reported a family of volatile, stable aluminum compounds.[9] This ligand has a five-membered ring linking one chelate nitrogen to the "bridgehead" (i.e., quaternary) carbon of the amidinate, thus preventing CDI deinsertion. Likewise, the ligand has been synthesized to allow control over the number of β -hydrogens, resulting in a series of four related copper(I) iminopyrrolidinates (Scheme 1). Herein we introduce two

Scheme 1. Series of Amidinate-Type Ligands with Differing Numbers of ß-Hydrogens, Shown As Their Corresponding Copper(I) Compounds

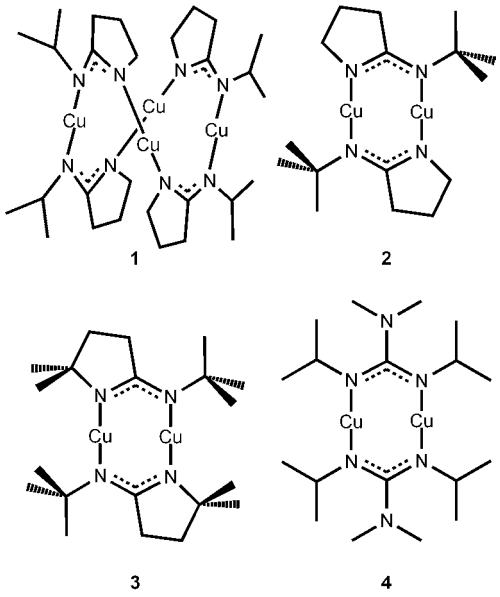

novel copper iminopyrrolidinates (copper(I) isopropyl-iminopyrrolidinate, **1** and copper(I) *tert*-butyl-iminopyrrolidinate, **2**) to complement our previously reported copper(I) *tert*-butyl-imino-2,2-dimethylpyrrolidinate (**3**),[10] and copper(I) *N*′,*N*″-diisopropyl-*N*,*N*-dimethyl guanidinate (**4**). A thorough exploration of the thermal chemistry of these four compounds was made to demonstrate how the redesign of this ligand has influenced thermal behavior. We have investigated the thermal stability of this series in the solid phase using a variety of thermogravimetric (TG) methods, as well as in solution phase using high resolution ^{1}H NMR of sealed tubes that have been treated at elevated temperatures to study decomposition kinetics. Finally, because of the superior thermal stability of **3**, we have undertaken an extensive study of the nature of the chemisorbed species produced on silica by **3** as deposited at 275 °C and when annealed at 350 °C.

RESULTS AND DISCUSSION

The copper compounds **1** and **2** were simply made by salt methathesis of copper(I) chloride with the in situ generated lithium iminopyrrolidinates. These compounds were isolated as white crystalline materials in moderate to high yields. Similarly, a recent paper describes trimeric, heteroleptic copper(I) guanidinates isolated from the attempted synthesis of $[Me_2NC(N^tBu)_2Cu]_2$.[11] We believe the ring of the iminopyrrolidinates reported herein was necessary to slightly reduce the steric bulk and permit the isolation of **2** as a dimeric species (see below).

The ^{1}H NMR of **2** was simple, suggesting a symmetrical oligomeric solution structure, similar to known copper guanidinate dimers.[6] However, compound **1** showed a more complex ^{1}H NMR. The doublets for the methyls of the isopropyl moiety in **1** suggested several environments. It is unclear if these multiple environments were due to an equilibrium of oligomers or from asymmetry in the molecule, but the relative integrations of these doublets were dependent on the concentration of **1**. Serial dilution of an NMR sample nor heating of the sample to 60 °C did not yield a trivial set of peaks similar to the spectra of **2**. The data from the ^{1}H NMR suggest that the species might be in an oligomeric equilibrium where the exterior proton environments are disordered in the structure, while the interior ring protons are more disordered. Fortunately, **1** could be isolated as X-ray quality crystals.

The structure of **1** shows a tetrameric arrangement in the solid state with an orthorhombic *Ccca* space group (Figure 2, Table 1). There are 16 tetramers in the unit cell, but only two that are crystallographically distinct. These molecules each have

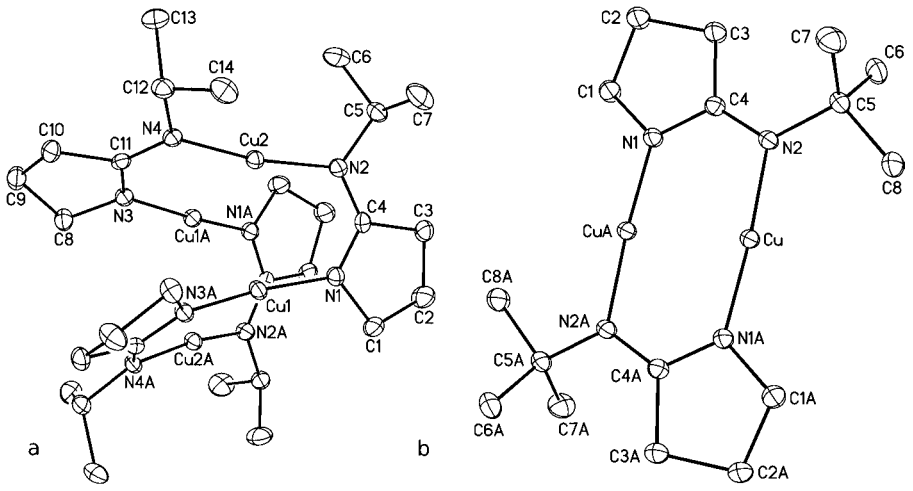

Figure 2. Structure of (a) **1** and (b) **2**, shown with the hydrogens removed for clarity. The thermal ellipsoids are at 30%.

dx.doi.org/10.1021/ic3021035 | *Inorg. Chem.* 2013, 52, 910−917

Table 1. Selected Bond Lengths and Angles for 1 and 2

compound 1		compound 2	
selected bond	length (Å)	selected bond	length (Å)
Cu1−Cu2	2.76	Cu−Cu	2.48
Cu1−Cu1a	3.00	Cu−N1	1.86
Cu1−N1	1.87	Cu−N2	1.89
Cu1−N3	1.86	N1−C4	1.34
Cu2−N2	1.89	N2−C4	1.33
Cu2−N4	1.89		
N1−C4	1.31		
N2−C4	1.34		
N3−C11	1.31		
N4−C11	1.33		
N1−C1	1.44		
N2−C5	1.46		
N3−C8	1.46		
N4−C12	1.49		
compound 1		compound 2	
selected angle	angle (deg)	selected angle	angle (deg)
Cu2−Cu1−Cu2	114.2	N1−Cu−N2	175.3
Cu2−Cu1−Cu1	57.1	N1−C4−N2	122.1
N3−Cu1−N1	170.5		
N2−Cu2−N4	170.7		
N1−C4−N2	123.8		
N3−C11−N4	123.6		

a core of four copper atoms that lay in a rhombohedral plane, with the rhombus of one molecule centered perpendicular to a C2 axis (with a minor torsion angle of 1.31°), and the other parallel to a different C2 axis (with a torsion angle of 0°). The closest Cu−Cu contact in the unit cell is 2.76 Å, which suggest there is no significant Cu−Cu interactions.[12] This is supported by the fact that the N−Cu−N bonds only deviate from linearity by about 10°, which is likely caused by steric hindrance in the ligands (see below). Since the connectivity of the molecules in the unit cell is very similar, only one molecule will be discussed in depth.

Interestingly, the two ligands bonded to any specific copper are bonded through the same type of nitrogen. For example Cu1 is bonded to the ring nitrogens N1 and N3, where one might expect the ligands to alternate. Additionally, the isopropyl groups of the ligand are all oriented toward the copper plane. These observations suggest that there is a fine balance of steric interference across the copper plane allowing a tetramer to form. This structure type has been seen previously for group 11.[13] The Cu−N bonds in this molecule have an average length of 1.88 Å, which is the same as in **3**.[10]

Considering the ligands oriented parallel to each other and on the same side of the copper plane, it is obvious that more crowding exists here. The ligands bend out slightly from one another, on average 26.5° from parallel. As well, there is a slight twist of about 6° across each ligand with respect to the line defined by the coppers which bind them.

The metallocycle C−N bonds are all about equivalent in this molecule (1.31 Å−1.34 Å), suggesting complete delocalization of the double bond, similar to **3**. The ligand's bridging N−C−N angle is about 123°, which is slightly larger than **3** and **4**.[6] This is quite understandable in the case of the tetramer, however, since the ligand is bridging a significantly large Cu−Cu distance.

The structure of **2** is more typical of the expected dimeric structures, considering **3** and **4** (Figure 2, Table 1). It crystallized in the monoclinic $P2_1/c$ space group with two molecules in the unit cell centered on inversion centers, where both molecules in the unit cell are identical. The Cu−Cu distance is ∼2.5 Å, which is significantly closer than in **1**. The copper geometry is very close to linear, contorting by 4.7° to lengthen the Cu−Cu bond. The metallocycle core is planar with the core N−C bonds all essentially equivalent (1.33 Å−1.34 Å), suggesting that the inherent double bond character is delocalized between these two bonds.

The thermolyses of **1** and **2** are quite encouraging. Compound **1** showed low residual mass using thermogravimetric (TG) analysis, and a single feature in weight loss, suggesting that the species volatilized easily. This low residual mass was surprising. Not only does this compound possess β-hydrogen atoms for abstraction, but the tetrameric structure was expected to yield a lower vapor pressure from increased molecular mass. It is possible that there exists an oligomeric equilibrium that allows **1** to volatilize as a lower order oligomer (mass spectral analysis shows a dimer), thus providing a larger vapor pressure at lower temperature. This also explains why **1** has a similar onset of volatilization to the dimeric compounds **3** and **4**.

Compound **2** showed more complex behavior. The residual mass was 28.1%, which was close to the percent mass of copper (31.3%) in this compound. The residual mass was confirmed to be metallic copper by powder X-ray diffraction, suggesting that **2** undergoes a low temperature reduction to produce Cu(0). This has previously been observed in the case of both **4** and the copper amidinates.[4] Because of the presence of the exocyclic pyrrolidine ring, the more favorable path for this thermal decomposition is β-hydrogen elimination rather than CDI deinsertion. This can be rationalized considering the crystal structure of **2**. The distortion of the dimer core and lack of

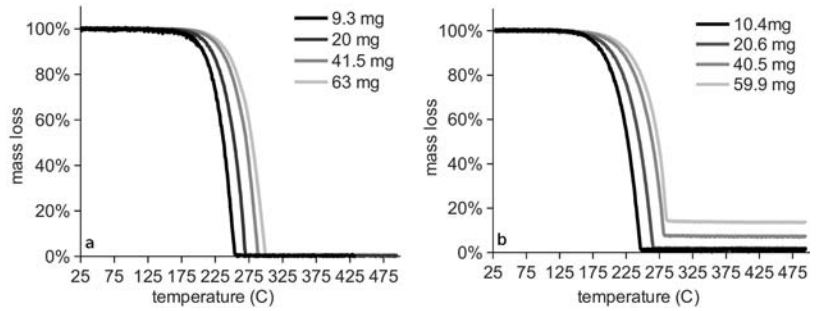

Figure 3. Thermal stress test of compounds (a) **3** showing no change in residual mass with increasing sample mass, and (b) **1**, showing increasing residual mass with increasing initial sample mass.

dx.doi.org/10.1021/ic3021035 | Inorg. Chem. 2013, 52, 910−917

steric protection exposes the copper and enables it to interact with the β-hydrogen atoms of neighboring molecules.

These compounds were also investigated by a thermal stress test using TG analysis. Essentially, a compound is measured using the same temperature ramp rate (10 °C/min) but using different sample masses. Thus, more sample would see higher temperatures because of the kinetics of thermolysis or volatilization. This valuable test can be used to gauge the behavior of the compound with respect to thermal handling during a deposition process, whether in the source bubbler or during the volatilization and entrainment to the deposition zone. A good example of this is the thermal stress test of **1** (Figure 3b). Compound **1** was shown to have a higher residual mass as the initial pan loading of the TG was increased. This indicated that it underwent decomposition as more compound was exposed to higher temperature. Compound **3** (Figure 3a) was seen to undergo no decomposition as pan loading was increased, demonstrating a superior thermal stability.

The residual mass trends of each compound **1**−**4** can be seen in Figure 4. It should be noted that the top sample mass that

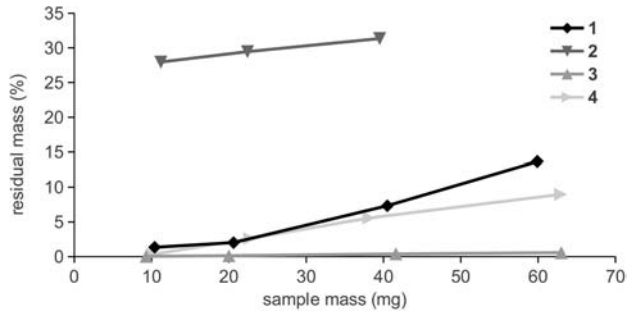

Figure 4. Thermal stress test trends for compounds **1**−**4**.

could be accommodated was about 65 mg; this filled the sample pan in all cases. With the exception of **1**, the stress trends are quite linear with an R^2 of 0.99. Compound **1** showed a higher deviation from linearity with an R^2 of 0.97. This might be due to a higher preponderance of a dimeric rather than tetrameric species at higher temperature, caused by a shift in oligomer equilibrium.

Compounds **1** and **4** show the most stress, deviating from a negligible residual mass at low loadings to quite high residual masses (13.7% for **1** and 9.0% for **4**) at high loadings. It is not surprising that these two compounds show similar thermal stress, since they both bear an isopropyl group for β-hydrogen elimination although CDI deinsertion cannot be ruled out in the case of **4**.

Compound **2** again showed poor thermal behavior with very high residual masses. Indeed, the highest loading was not attempted for **2** since the 39.5 mg of sample gave 31.35%, which is the mass percent of copper in that compound (31.32%). This was not surprising, given the high residual mass seen previously. This reactivity stands out because **2** can be considered of intermediate reactivity with respect to number of β-hydrogens within this family. However, it has a dimeric structure (unlike **1**, which exists in the solid as a tetramer) and so is less sterically protected at the copper centers. This would lend it worse thermal stability.

Compound **3** showed very good thermal stress resistance, rising only to 0.56% residual mass at 63.0 mg sample mass. This supports our hypothesis that **3** will be the most thermally stable of this series of compounds because of its lack of reactive hydrogens and the robust nature of the core of this ligand with respect to CDI deinsertion.

Using TG analysis, the evaporation kinetics were evaluated for **1**−**4** (Figure 5). Compound **4** showed the highest

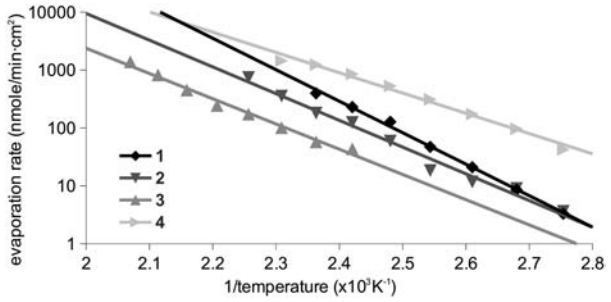

Figure 5. Evaporation kinetics of **1**−**4** by TG analysis.

evaporation at the lowest temperatures. Compounds **1** and **2** showed similar evaporation kinetics within the temperatures studied. This is unsurprising since **1** and **2** are expected to both volatilize as dimers and have similar molecular masses (a mass difference of only two methyl groups). Surprisingly, **3** showed the slowest evaporation kinetics even though it has a mass close to that of **4**. It is possible that the measured evaporation kinetics of the copper(I) iminopyrrolidinates are slower than **4** because of the more rigid framework of the iminopyrrolidinate ligand. The rigidity of the ligand would cause a compact, planar structure and allow for stronger intermolecular attraction within the solid. Additionally, the copper(I) iminopyrrolidinates would be expected to have less entropy gain during volatilization than **4**: the rigid ligand has fewer bonds that are free to rotate in the gas phase than in the solid state, compared to the relatively less constrained guanidinate of **4**. From the isothermal TG analysis and using the Langmuir equation,[14] the temperatures at which 1 Torr of vapor pressure was obtained was estimated to be 158 °C, 161 °C, 187 °C, and 125 °C for **1**−**4**, respectively.

To further illuminate the thermal chemistry of these compounds, they were each sealed in heavy walled NMR tubes and heated in an oven at 165 °C over a period of days. An ^{1}H NMR was collected each day to observe their thermal decomposition (Figure 6, Table 2). Compound **4** revealed decomposition to produce diisopropylcarbodiimide, as previously seen.[6] The decomposition of **4** that followed first order decomposition kinetics and had a calculated half-life of 33.8 h. The parent guanidine was also observed as a product of thermolysis, and its origin of production is discussed below.

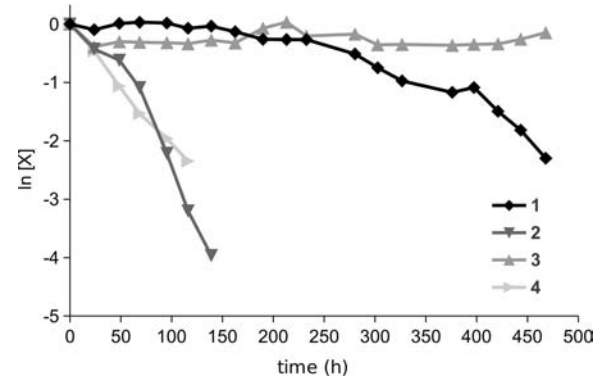

Figure 6. Thermal decomposition of **1**−**4** at 165 °C over 21 days.

dx.doi.org/10.1021/ic3021035 | *Inorg. Chem.* 2013, 52, 910−917

Table 2. Kinetic Data for the Thermal Decomposition of 1−4 at 165°C[a]

compound	rate constant (s^{-1})	calculated half-life (h)	correlation coefficient
1	1.06×10^{-6}	181.1	0.902
2	8.14×10^{-6}	23.7	0.944
3	no measurable decomposition		
4	5.69×10^{-6}	33.8	0.995

[a]The "correlation coefficient" refers linear fit in Figure 10.

Compound **1** showed much better thermal behavior than **4**, as was expected from the TG data. The compound decomposed following first order kinetics with a half-life of 181.1 h, and there was very obvious plating of copper on the NMR tube walls. The main byproduct from the thermolysis was the parent ligand, isopropyliminopyrrolidine. There was no evidence of CDI nor any evidence of oxidized ligand. There was an obvious flocculant in the NMR tube after the thermolysis; this might be the oxidized ligand wherein a proton was lost. Compound **2** showed similar decomposition to **1**, but much more quickly ($t_{1/2}$ = 23.7 h). The NMR tube was again obscured with plated Cu(0) and had a flocculant precipitate, and the ^{1}H NMR showed free, protonated ligand. It is possible that since **1** forms a tetramer, this imparts thermal stability to the compound, perhaps because the tetramer has to dissociate to a smaller oligomer to thermalize. This would also account for the relatively poor linear fit to first order kinetics: if the tetramer forms at higher concentration, then there would be a slightly higher rate of decomposition as the overall concentration of **3** dropped and the dimer-tetramer equilibrium began to favor the dimer.

The full mechanism that produces the protonated ligand remains unclear. We propose β-hydrogens as the most likely source for protons for the origin of free ligand. Surface work by Gordon and Zaera[4] found that butene elimination occurs from copper(I)-*N*,*N*′-di-*sec*-butylacetamidinate leaving an N−H moiety, which might be another source for protons. However, no ^{1}H signals were observed in the NMR tube thermolysis experiment that suggest a similar mechanism occurring here. Evidence for disproportionation of Cu(I) acetamidinates has also been demonstrated in surface studies on SiO_2 substrates.[15] Since disproportionation of Cu(I) to Cu(II) and Cu(0) is a common thermolysis route for Cu(I) compounds, we offer the following insight. We observed a blue color imparted to **2** during the solution based ^{1}H NMR thermolysis study (Figure 10), suggesting the formation of a Cu(II) species. Attempts to isolate a Cu(II) compound by crystallization failed and resulted only in the isolation of crystals of **2** with a blue impurity. Interestingly, we previously had prepared oxidized guanidine (i.e., the product of β-hydrogen elimination) from the reaction between guanidine and a Cu(II) compound.[7] Therefore, a Cu(II) intermediate might be involved in β-hydride abstraction thermolysis for this class of compound. We are continuing to study the thermolysis mechanisms of these compounds to gain a fuller understanding of this complicated thermal behavior.

Compound **3** showed no decomposition at 165 °C over 21 days. It was expected that its ligand (with no β-hydrogens and without the CDI deinsertion pathway) would impart the best thermal stability; however, this marked difference was surprising. To further explore this, **3** was subjected to a rigorous surface study. This study used a combination of solid-state nuclear magnetic resonance (SS-NMR), elemental analysis, and high-resolution NMR (HR-NMR) to determine the initial monolayer and surface chemistry of **3** on high-surface area silica. SS-NMR has been shown to be a useful tool in analysis of initial adsorption complexes on high-surface area substrates.[16,17]

Approximately 1 g of high surface area silica was loaded into a reactor and annealed under vacuum at 350 °C for about 16 h prior to exposure to precursor. This ensured a consistent hydroxyl density at the surface between each experiment. Under these conditions, silica is expected to have a hydroxyl density of 2−3.5 OH/nm^2.[18] A bubbler temperature of 165 °C has been show to produce a sufficient vapor pressure for **3** so this temperature was used for all experiments.[10] A deposition temperature of 200 °C was attempted but it was determined that the precursor did not react with the silica. When the silica that was exposed to vaporous **3** was washed with D_2O, only unreacted, dimeric precursor was found at this temperature, suggesting that **3** was simply physisorbed. This was quite interesting, since it demonstrated the stability of **3**: it was stable in aqueous solution for several hours, which was not an anticipated characteristic of this precursor. As well, it existed in a physisorbed state on the silica surface for up to 17 h without decomposing or significantly desorbing.

It was found that a temperature of 275 °C was needed to chemisorb **3**. There are three main experiments that will be discussed: sample **a** is unmodified silica, sample **b** has undergone chemisorption of **3**, and sample **c** has undergone chemisorption of **3** with a subsequent anneal at 350 °C for 4 h. Energy-dispersive X-ray spectroscopy (EDX) showed the presence of copper on samples **b** and **c**. No copper was detected on sample **a**, as expected. Interestingly, when **b** was allowed to sit in air, it changed color to turquoise-green within 15 min. This is likely a conversion of the as-deposited surface species to a hydrated copper oxide.

^{1}H/X Cross-polarization magic angle spinning solid-state NMR (CP/MAS SS-NMR) was used as the primary method of characterization for the samples **a**−**c**. The benefit of this technique is that the observed signals originate only from nuclei that are in close proximity to protons; in these samples, this means surface species only. The ^{29}Si CP/MAS SS-NMR spectra of samples **a**−**c** showed typically silica signals (Figure 7).[19] In **a**, there are signals at around −101.6 ppm, −110.5 ppm and a shoulder at −92 ppm. The signal at −101.6 ppm is attributed to silanol groups (||-Si−OH) at the surface while the signal at −110.5 ppm is attributed to fully dehydroxylated silicon near the surface of the bulk sample (||-Si). The shoulder at −92 ppm arises from silandiol species at the surface (||-Si(OH)$_2$).

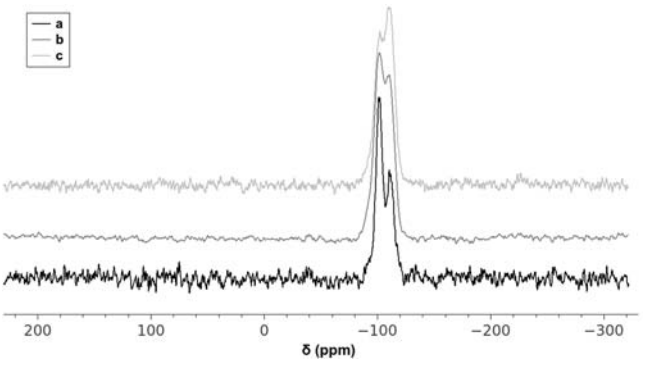

Figure 7. Solid-state ^{29}Si {^{1}H} CP/MAS NMR of samples **a**−**c**.

dx.doi.org/10.1021/ic3021035 | *Inorg. Chem.* 2013, 52, 910−917

The middle trace in Figure 7 shows the ^{29}Si CP/MAS SS-NMR spectrum for **b**. It is apparent that the only signals present are similar to those of the unmodified silica. Indeed, the lack of other signals demonstrated that chemisorbed precursor interacts with the silica through an oxygen atom, rather than forming direct precursor-silicon bonds. That is, the precursor likely chemisorbs through a ||-Si−O−Cu interaction, rather than a ||-Si−Cu or ||-Si−N. As well, the relative intensities of the various Si species present at the surface differ from that of **a**. The silidiol shoulder vanished in **b**, and the relative intensity of the silanol peak decreased in **b** compared to **a**. Thus, the active surface hydroxyl groups are being consumed as precursor is taken up by the silica surface. However, the continued presence of a hydroxyl signal showed that saturation has not been reached under these experimental conditions.

The ^{13}C CP/MAS SS-NMR spectra of samples **a**−**c** were diagnostic of the nature of the surface species (Figure 8). As

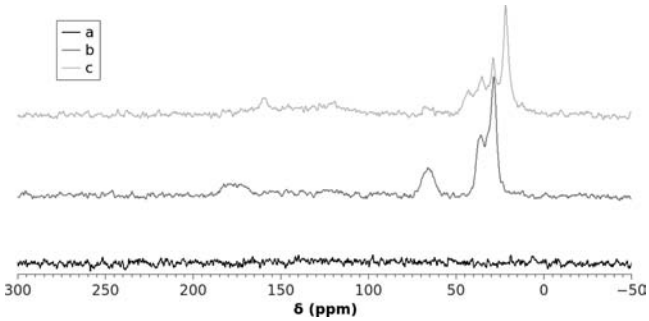

Figure 8. Solid-State ^{13}C {^{1}H} CP/MAS NMR of high surface area silica samples **a**−**c**.

expected, **a** did not show any carbon signals, and highlights the lack of carbon impurities at the silica surface before exposing the system to precursor. The trace for **b** gave four clear signals centered at 28.5, 35.8, 65.9, and 176.5 ppm. The signal at 176.5 ppm was attributed to the quaternary carbon between the two chelating nitrogens on the iminopyrrolidinate ligand. The broadening of this peak was likely due to the rigidity of the ligand in the chemisorbed surface species. This caused an incomplete averaging of the dipolar and scalar coupling at the 4.5 kHz MAS spinning speed used. The signal at 65.9 ppm came from the quaternary carbon in the iminopyrrolidinate ring. The quaternary carbon from the *tert*-butyl substituent likely contributed to this peak as well. This peak has a similar broadening to the previous peak. The sharp signals 28.5 ppm and 35.8 ppm were due to the methyl substituents attached to the ring and the methylene carbons that are part of the ring in the iminopyrrolidinate ligand respectively. The methyl groups on the *tert*-butyl substituent would appear in the same range as these peaks and so were likely buried therein. The assignment of these peaks agreed with the ^{13}C HR-NMR reported for the pure compound **3**.[10]

Elemental analysis for carbon, hydrogen, and nitrogen was also performed on samples **a**−**c** (Table 3). Given the assumed hydroxyl density at the surface of 2−3.5 hydroxyls/nm^2, the elemental analysis showed about 60% saturation of the surface, corroborating evidence from the ^{29}Si SS-NMR. To give more insight into the nature of the surface species present, a molar ratio of each element was determined relative to nitrogen, which was fixed at 2 to represent the stoichiometry of nitrogen in the ligand. Given the molar ratios, the majority of the ligand

Table 3. Elemental Analysis Samples a−c[a]

		sample **a**	sample **b**	sample **c**
C	wt %	<0.3	2.71	4.16
	mole ratio		7	7
H	wt %	<0.3	0.59	0.79
	mole ratio		17	16
N	wt %	<0.3	0.95	1.40
	mole ratio		2	2

[a]The data for sample **a** were below the limit of detection.

appeared to be intact on the surface. However, the carbon ratio is lower than expected for a completely intact ligand, which can be explained by the loss of a fragment as large as C_4 from the ligand upon surface adsorption.

To further elucidate the adsorption mechanism a small amount of sample **b** was washed with D_2O to etch off the chemisorbed surface species for study using HR-NMR (Figure 9, bottom trace). This relatively clean spectrum shows that all

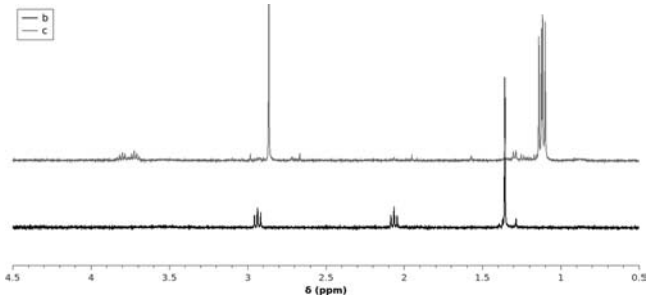

Figure 9. High-resolution ^{1}H NMR of D_2O after it was washed over samples **b** and **c**.

the peaks from the surface species match what is known for the iminopyrrolidinate ligand, with an absence of the signal for the methyl groups from the *tert*-butyl substituent. This concretely demonstrate that the *tert*-butyl substituent was eliminated upon initial surface adsorption at 275 °C. The somewhat higher hydrogen ratio likely had a contribution from the silica hydroxyl groups, which dehydrated during the combustion analysis.

The thermal stability of the initial chemisorbed species was examined by annealing **b** at 350 °C for 4 h under vacuum, producing sample **c**. The ^{13}C CP/MAS SS-NMR for **c** gave a spectrum that was somewhat similar to that of **b** (Figure 8). However, the quaternary carbon signal originally at 176.5 ppm was not present, and a new quaternary carbon signal appeared at 160 ppm. The other quaternary carbon signal present in **b** also appeared for **c** with a considerably weakened intensity from the annealing process. Two new carbon signals have appeared at 10 and 45 ppm, confirming that a new surface species forms. The ^{29}Si CP/MAS SS-NMR spectrum for **c** was very similar to unmodified silica (Figure 7). Even at temperatures as high as 350 °C, no alkylation of the silicon occurred at the surface, and any thermolyzed chemisorbed species were still bonded through a ||-Si−O-R type interaction. Again, there was a change in the intensity of the peaks originating from each silica environment. Similar to the signal from **b**, the intensity of the silanol species at the surface decreased with respect to the signal for completely dehydroxylated silicon. This is likely due to the participation of silanol protons in the decomposition mechanism of the chemisorbed species from **b**.

dx.doi.org/10.1021/ic3021035 | *Inorg. Chem.* 2013, 52, 910−917

Similar to the study done for **b**, a small of amount of **c** was washed with D_2O and examined via ^1H HR-NMR (Figure 9, top trace). Similar to the ^1H HR-NMR of **b**, the spectrum for **c** was very clean and exhibited only one species. There were two doublets and two septets, representing iso-propyl groups. There was an isolated singlet which integrated to two protons relative to the isopropyl group. This singlet is too shielded to be an imine group (like $^iPrN{=}CH_2$), and thus it could be that both nitrogen atoms remain in the surface species to form a methylene diimine. A mass spectral analysis of a (non-deuterated) aqueous solution found a peak at 89 amu, which is the mass of this surface species with an additional proton. Using a hybrid quadrupole time-of-flight mass spectrometer, the fragmentation of this parent ion supported the formulation $^iPrN(H)CH_2NH_2$ (Figure 10). Thus, the ring methyls become

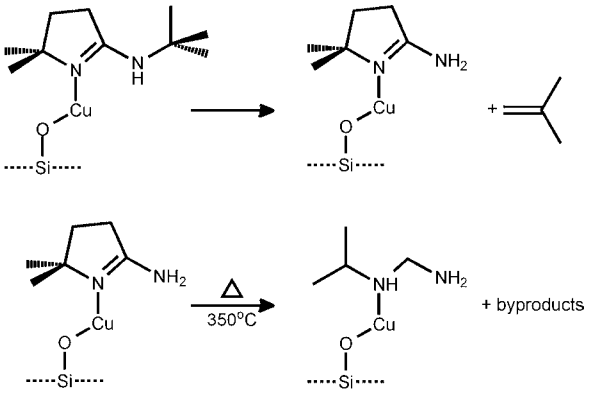

Figure 10. Possible thermolysis of the surface species formed by **3** on high-surface area silica.

the methyls of an isopropyl group, and the quatenary carbon is protonated to produce a methylene. Interestingly, Chabal et al. also suggest a diamine as a stable surface species during ALD of Cu metal on SiO_2 substrates.[15] Combustion analysis of **c** did not clarify the formulation, giving very similar carbon, hydrogen, and nitrogen molar ratios to that of **b** (Table 3). A more rigorous surface study is planned to clarify the 350 °C thermolysis mechanism.

CONCLUSION

A series of copper(I) iminopyrrolidinates were synthesized and evaluated by thermogravimetric analysis and in C_6D_6 solutions by ^1H NMR to determine their thermal stability and suitability as precursors in CVD processes. The employed asymmetric, cyclic amidinate ligand proved to impart excellent thermal stability when no β-hydrogens were present. A direct comparison of the number of β-hydrogens to thermal stability was complicated by the tetrameric structure of **1**, which was thought to influence thermal stability.

A valuable thermal stress test by TGA was devised and provided complementary thermal stability trends to solution based thermolysis studies. Advantages of the thermal stress test by TGA were faster data collection and use of conditions more pertinent to CVD processes. The solution based thermolysis studies identified the parent amidine and copper metal as thermolysis products of **1** and **2**. The amidines were produced through an intramolecular hydrogen abstraction, and a β-hydride abstraction mechanism was proposed. Compound **3** showed negligible decomposition in both the TGA and the solution experiments, and is an excellent candidate for copper deposition experiments.

An extensive surface reactivity study of **3** was undertaken, revealing some interesting thermal behavior. Compound **3** lost an alkyl group on chemisorption at 275 °C, but was stable to thermolysis up to 350 °C, demonstrating that the design of the ligand system did indeed protect the monolayer from thermolysis. At 350 °C, the surface species underwent further thermolysis by an unknown mechanism to produce a surface species suspected to be the methylenediamine $^iPrN(H)$-CH_2NH_2.

EXPERIMENTAL SECTION

General Considerations. All manipulations involving the synthesis and handling of copper(I) compounds were performed in a nitrogen filled drybox. The chemicals CuCl and 2.5 M BuLi in hexanes were purchased from Aldrich Chemical Co. and used as received. All solvents used in manipulation of copper(I) compounds were ACS grade and purified from an Mbraun Solvent Purifier System. All other solvents were ACS grade and used as received. Nuclear Magnetic Resonance was done on 300 MHz Avance 3 and 400 MHz Bruker AMX. Canadian Microanalytical Service Ltd. performed combustion analyses. Thermogravimetric analysis was performed on a TA Instruments Q50 apparatus located in an MBraun Labmaster 130 Drybox under a nitrogen atmosphere. Isopropyl-iminopyrrolidine and *tert*-butyl iminopyrrolidine were prepared by literature procedures.[9]

Copper(I) Isopropyl-iminopyrrolidinate (1). Isopropyl-iminopyrrolidine (5.11 g, 40.49 mmol) was partially dissolved in 60 mL of Et_2O and cooled to 0 °C in an ice bath. A 16.2 mL portion of butyl lithium was added dropwise, and a suspension formed after stirring for 2 h. In a separate flask, CuCl (4.2 g, 42.42 mmol) was suspended in 60 mL of tetrahydrofuran (THF) and cooled to 0 °C in an ice bath. The suspension of lithium isopropyl-iminopyrrolidine was added via cannula to the cooled suspension of CuCl and was then allowed to warm to room temperature and stirred overnight. The volatiles were removed from the reaction flask by reduced pressure, and the remaining solid was stirred in 100 mL of toluene for 10 min. The cloudy solution was filtered, and the clear filtrate was concentrated under vacuum and kept at −35 °C for 2 days. A mass of small, needle crystals was collected by filtration, washed with pentane, and then dried under vacuum to afford 5.03 g, 65.8%. Mp 138 °C. ^1H NMR (400 MHz, C_6D_6): δ 3.49, δ 3.24 (m, 1H, $NCH(CH_3)_2$); δ 3.34, δ 3.26 (t, 2H, $NCH_2CH_2CH_2C$); 2.04 (t, 2H, $NCH_2CH_2CH_2C$); δ 1.58 (quintet, 2H, $NCH_2CH_2CH_2C$); δ 1.487, δ 1.304, δ 1.208, δ 1.158 (d, 6H, $NCH(CH_3)_2$). ^{13}C NMR (300 MHz, C_6D_6) δ 179.84, δ 175.38, δ 54.19, δ 53.30, δ 53.15, δ 51.19, δ 50.48, δ 50.00, δ 29.02, δ 28.69, δ 28.65, δ 27.70, δ 27.55, δ 27.39, δ 27.36, δ 24.99, δ 24.72, δ 24.64. Combustion analysis, found (calculated): C, 44.63(44.55); H, 7.11(6.94); N, 14.84(14.84).

Copper(I) *tert*-Butyl-iminopyrrolidinate (2). *tert*-Butyl iminopyrrolidine (1.72 g, 12.26 mmol) was dissolved in 60 mL of THF. A 4.9 mL portion of 2.5 M butyl lithium was added, and the solution was stirred for 2 h. CuCl (1.25 g, 12.62 mmol) was added in one portion, and the suspension was stirred overnight. Volatiles were removed under reduced pressure, and the remaining solid was taken up in THF and filtered. The filtrate was concentrated and then kept at −35 °C for 1 day. Colorless, block crystals were collected by decanting the solution, washing with pentane, and then drying under vacuum; obtained 1.59 g, 63.9%. Mp 148 °C. ^1H NMR (300 MHz, C_6D_6): δ 3.25 (t, 2H, $NCH_2CH_2CH_2C$), δ 2.19 (t, 2H, $NCH_2CH_2CH_2C$), δ 1.63 (quintet, 2H, $NCH_2CH_2CH_2C$), δ 1.32 (s, 9H, $NC(CH_3)_3$). ^{13}C NMR (300 MHz, C_6D_6): δ 180.01 ($NCH_2CH_2CH_2C$), δ 52.45 ($NCH_2CH_2CH_2C$), δ 33.72 ($NC(CH_3)_3$), δ 33.26 ($NC(CH_3)_3$), δ 31.64 ($NCH_2CH_2CH_2C$), δ 26.33 ($NCH_2CH_2CH_2C$). Combustion analysis, found (calculated): C, 47.08(47.39); H, 7.49(7.46); N, 13.69(13.82).

Crystallography. X-ray structural analysis for **1** and **2**: Crystals were selected and mounted on plastic mesh using viscous oil flash-

dx.doi.org/10.1021/ic3021035 | *Inorg. Chem.* 2013, 52, 910−917

cooled to the data collection temperature. Data were collected on a Bruker-AXS APEX CCD diffractometer with graphite-monochromated Mo−Kα radiation (λ = 0.71073 Å). Unit cell parameters were obtained from 60 data frames, 0.3° ω, from three different sections of the Ewald sphere. The systematic absences in the data and the unit cell parameters were uniquely consistent to *Ccca* for **1** to *P*21/*c* for **2**. The data sets were treated with SADABS absorption corrections based on redundant multiscan data.[20] The structures were solved using direct methods and refined with full-matrix, least-squares procedures on F^2. The compound molecules were each located on an inversion point in **2**. Two symmetry unique but chemically identical molecules of the compound in **1** are each located on a 2-fold rotation axis: in one case the 2-fold axis is parallel to the N−Cu−N axis and in the other case the 2-fold axis is perpendicular to the N−Cu−N axis bisecting the Cu atoms on the opposite distal positions of the tetracopper rhombus. One THF solvent molecule of crystallization per two tetrameric complexes in **1** was located severely disordered and treated as diffused contribution.[21] One isopropyl group in **1** was located disordered with a 23/77 refined occupancy ratio. Chemically equivalent bond distances and angles in the disordered group were restrained to average values with equal atomic displacement atomic parameter contraints on equivalent atoms. All non-hydrogen atoms were refined with anisotropic displacement parameters. All hydrogen atoms were treated as idealized contributions. Atomic scattering factors are contained in the SHELXTL 6.12 program library.[20]

Surface Exposure Experiments. The exposure experiments were performed in a home-built reactor. The reaction chamber consisted of a stainless steel ring support covered in 200 stainless steel mesh with a plug of glass wool to prevent loss of silica powder. The system had one inlet from a heated bubbler and one inlet for He (purity of 99.999%). All fittings used in this system were either CF or VCR to ensure a high-vacuum seal. The system was leak checked using a gas thermal conductivity/leak detector (Gow-Mac Instrument Co.) and an overpressure of He. For the exposure experiments, typically about 1 g of high surface area SiO_2 powder (EP10X; PQ Corporation; 300 m^2/g S.A.; 1.8 cm^3/g P.V.; 24 nm P.S.; 100 μm P.D.) was used. The powder was pretreated in the reactor at 350 °C for 16 h under vacuum before exposure to the precursor. The reactor and lines were heated to temperature and allowed to equilibrate for 1−2 h before introduction of the precursor. The precursor (typically 0.6−0.8 g) was then vaporized and transported to the substrate with the system under 10^{-3} Torr vacuum. The substrate was exposed to volatilized precursor for 17 h before the system was cooled to room temperature for handling. Both precursor and substrate were handled in inert atmosphere.

Annealing experiments were performed in a tube furnace while under vacuum. Samples were loaded into the furnace under a blanket of nitrogen gas. Samples were annealed for 2 h.

Characterization of Surface Species. Solid-state NMR experiments were performed at 4.7 T on a Bruker Avance III console. All spectra were obtained using a Bruker 7 mm ^{1}H/X/Y probe. ^{13}C (ν_0 = 50.3 MHz) cross-polarization magic angle spinning (CP/MAS) experiments were collected at a spinning rate of 4.5 kHz using a 3.4 μs 90° proton pulse with a contact time of 2 ms where the contact pulse was ramped on the ^{1}H channel. A relaxation delay of 2 s was sufficient to prevent saturation and typically total acquisition times were 16−30 h. Glycine was used as an external secondary reference for the ^{13}C chemical shift scale. Spectra were treated with 40 Hz line broadening during processing. ^{29}Si (ν_0 = 39.7 MHz) CP/MAS experiments were collected at a spinning rate of 4.5 kHz using a 3.85 μs 90° proton pulse with a contact time of 10 ms where the ^{1}H channel contact pulse was ramped. The relaxation delay was 2 s and typically required 2−8 h acquisition times. TMSS was used as an external reference for the ^{29}Si chemical shift scale. Spectra were treated with 30 Hz line broadening during processing. All spectra were obtained with high power proton decoupling during acquisition.

Samples were prepared for High Resolution NMR (HR-NMR) by adding a small amount, typically 40−50 mg, of modified silica powder to 2 mL of D_2O (Sigma), agitating, and allowed to sit for 15 min. The D_2O solution was then decanted and studied via HR-NMR. d_4-TSP was used as an internal reference.

Electron dispersive X-ray spectroscopy (EDX) was performed on the modified silica samples as qualitative proof for the presence of copper. Samples were mounted on an aluminum support using carbon tape and loaded into a Tescan Vega II SEM equipped with an Oxford Inca 200 EDX for analysis.

AUTHOR INFORMATION

Corresponding Author

*Tel: +1 613-520-2600, ext. 2244. E-mail: sean_barry@carleton.ca.

Notes

The authors declare no competing financial interest.

REFERENCES

(1) 2011 Edition of the International Technology Roadmap for Semiconductors; http://www.itrs.net/Links/2011ITRS/Home2011.htm.

(2) (a) Li, Z.; Rahtu, A.; Gordon, R. G.. *J. Electrochem. Soc.* **2006**, *153*, C787. (b) Li, Z.; Barry, S. T.; Gordon, R. G. *Inorg. Chem.* **2005**, *44*, 1728.

(3) Krisyuk, V.; Aloui, L.; Prud'homme, N.; Sysoev, S.; Senocq, F.; Samélor, D.; Vahlas, C. *Electrochem. Solid-State Lett.* **2011**, *14*, D26.

(4) (a) Ma, Q.; Guo, H.; Gordon, R. G.; Zaera, F. *Chem. Mater.* **2010**, *22*, 352. (b) Ma, Q.; Guo, H.; Gordon, R. G.; Zaera, F. *Chem. Mater.* **2011**, *23*, 3325.

(5) Turgambaeva, A.; Prud'homme, N.; Krisyuk, V.; Vahlas, C. J. *Nanosci. Nanotechnol.* **2011**, *11*, 8198.

(6) Coyle, J. P.; Monillas, W. H.; Yap, G. P. A.; Barry, S. T. *Inorg. Chem.* **2008**, *47*, 683.

(7) Coyle, J. P.; Johnson, P. A.; DiLabio, G. A.; Barry, S. T.; Muller, J. *Inorg. Chem.* **2010**, *49*, 2844.

(8) Tsuda, T.; Watanabe, K.; Miyata, K.; Yamamoto, H.; Saegusa, T. *Inorg. Chem.* **1981**, *20*, 2728.

(9) Wasslen, Y. A.; Kurek, A.; Johnson, P. A.; Pigeon, T. C.; Monillas, W. H.; Yap, G. P. A.; Barry, S. T. *Dalton Trans.* **2010**, *39*, 9046.

(10) Coyle, J. P.; Kurek, A.; Pallister, P. J.; Sirianni, E. R.; Yap, G. P. A.; Barry, S. T. *Chem. Commun.* **2012**, *48*, 10440.

(11) Willcocks, A. M.; Robinson, T. P.; Roche, C.; Pugh, T.; Richards, S. P.; Kingsley, A. J.; Lowe, J. P.; Johnson, A. L. *Inorg. Chem.* **2012**, *51*, 246.

(12) Cotton, F. A.; Daniels, L. M.; Feng, X.; Maloney, D. J.; Matonic, J. H.; Murilio, C. A. *Inorg. Chim. Acta* **1997**, *256*, 291.

(13) (a) Abdou, H. E.; Mohamed, A. A.; Fackler, J. P.; Jiang, X.; Bollinger, J. *J. Cluster Sci.* **2007**, *18*, 630. (b) Baik, M.-H.; Lee, D. *Chem. Commun.* **2005**, 1043. (c) Beck, J.; Strähle, J. *Angew. Chem., Int. Ed. Engl.* **1986**, *25*, 95.

(14) Kunte, G. V.; Shivashanker, S. A.; Umarji, A. M. *Meas. Sci. Tech.* **2008**, *19*, 025704.

(15) Dai, M.; Kwon, J.; Halls, M. D.; Gordon, R. G.; Chabal, Y. J. *Langmuir* **2010**, *26*, 3911.

(16) Haukka, S.; Lakomaa, E. L.; Root, A. *J. Phys. Chem.* **1993**, *97*, 5085.

(17) Wasslen, Y. A.; Tois, E.; Haukka, S.; Kreisel, K. A.; Yap, G. P. A.; Halls, M. D.; Barry, S. T. *Inorg. Chem.* **2010**, *49*, 1976.

(18) Bergna, H. E. *The Colloid Chemistry of Silica*; American Chemical Society: Washington, DC, 1994.

(19) Maciel, G. E.; Sindorf, D. W. *J. Am. Chem. Soc.* **1980**, *102*, 7606.

(20) Sheldrick, G. M. *Acta Crystallogr.* **2008**, *A64*, 112.

(21) Spek, A. L. *J. Appl. Crystallogr.* **2003**, *36*, 7.